Lab on a Chip

Femto-liter Nanofluidic Valve Utilizing Glass Deformation

Journal:	*Lab on a Chip*
Manuscript ID	LC-ART-12-2018-001340.R1
Article Type:	Paper
Date Submitted by the Author:	10-Mar-2019
Complete List of Authors:	Kazoe, Yutaka; The University of Tokyo, Pihosh, Yuriy; The University of Tokyo, Department of Applied Chemistry Takahashi, Hitomi; The University of Tokyo Ohyama, Takeshi; The University of Tokyo Sano, Hiroki; The University of Tokyo Morikawa, Kyojiro; The University of Tokyo, School of Engineering Mawatari, Kazuma; The University of Tokyo, Kitamori, Takehiko; The University of Tokyo,

Femto-liter Nanofluidic Valve Utilizing Glass Deformation

Yutaka Kazoe, Yuriy Pihosh, Hitomi Takahashi, Takeshi Ohyama, Hiroki Sano, Kyojiro Morikawa, Kazuma Mawatari and Takehiko Kitamori*

Department of Applied Chemistry, School of Engineering, The University of Tokyo, 7-3-1 Hongo, Bunkyo, Tokyo 113-8656, Japan. E-mail: kitamori@icl.t.u-tokyo.ac.jp; Fax: +81 3 5841 6039

Abstract

In the field of micro/nanofluidics, the channel open/close valves are among the most important technologies for switching and partitioning actions and integration of various operations into fluidic circuits. While several types of the valves have been developed in microfluidics, few are capable in nanofluidics. In this study, we proposed a femto-liter (fL) volume nanochannel open/close valve fabricated in glass substrates. The valve consists of a shallow, circular and stepped-bottom valve chamber connected to nanochannels and an actuator. Should even a tiny deformation occur at the nanolevel in glass, an open/close state of a nanochannel (10-1000 nm) can be achieved. We designed the fL-valve based on an analytical material deformation model, and developed the valve fabrication process. We then verified the open/close of the valve using a 308 fL valve chamber with a four-stepped nanostructure fitting an arc-shape of deflected glass, confirmed its stability and durability over 50 open/close operations, and

succeeded in stopping/flowing an aqueous solution at 209 fL/s under a 100 kPa pressure in a 900 nm nanochannel with a fast response of ~0.65 s. A leak flow from the closed valve was sufficiently small even at a 490 kPa pressure-driven flow. Since the developed fL-valve can be applied to various nanofluidic devices made of glass and other rigid materials such as plastic, it is expected that this work will contribute significantly to the development of novel integrated micro/nanofluidics chemical systems for use in various applications, such as single cell/single molecule analysis.

1. Introduction

The development of microfluidics has made possible miniaturized and integrated chemical systems for biochemical and environmental analysis, and chemical synthesis.[1,2] To integrate various microscale operations such as mixing, reaction and separation, referred to as micro unit operations (MUOs),[3] open/close channel valves for switching and partitioning are among the most important technologies. Several types of microchannel valves of nL-volumes exploiting channel deformations,[4] hydrogel structures,[5] and wettability patterns,[6] have already been developed. Among these, valves exploiting channel deformations have the most overall usability because they normally do not require surface modifications, chemical reactions, or specific structures that would narrow their applicability in microfluidic devices. Such valves have already been incorporated into devices made of polydimethylsiloxane (PDMS), which is soft enough to permit channel closure by microchannel deformation. Although the material's solubility to organic solvents and gas permeability restricts its use,

highly-integrated chemical systems where PDMS valve are implemented have already been demonstrated.[4,7-9]

Recently, the field has further downscaled from microfluidics to nanofluidics exploiting top-down fabricated 10^1–10^3 nm sized nanochannels,[10] which are distinguished from conventional nanotechnology based on bottom-up fabricated 10^0 nm sized nanotubes and nanopores. We have established a nanofluidic device platform where nanochannels are fabricated on a glass substrate.[11] By exploiting nanospaces with dominant surface effects and aL–fL volumes that are much smaller than a single cell, nano unit operations (NUOs) such as selective capture of countable-molecules[12] and fast proton transfer[13] have been developed. A highly-sensitive detection of non-fluorescent molecules in the nanochannel was also realized.[14] Based on these NUOs, we have developed chemical devices such as single-molecule ELISA,[15] aL-chromatography,[16] nano-heat pipe,[17] and light-driven fuel cell.[18] Other devices like a droplet based single-enzyme analysis[19] and an epigenetic analysis by single molecule sorting[20] have also been developed. Currently, highly-integrated chemical systems, such as a single cell/single molecule analysis system, are expected.

However, open/close valves for nanofluidic devices remains challenging. For 10^0 nm sized nanotube, an open/close valve controlled by silicon cantilevers was proposed. However, the volume is too small compared to aL–fL volumes, and the principle verification is limited to numerical simulation.[21] For 10^1–10^3 nm sized nanochannels, previously, we developed an fL-valve capable of exploiting dominant surface tension (Laplace pressure) and nanostructures, but the repeated switching and partitioning

operations required in highly-integrated systems are somewhat problematic.[22] Most recently, a nanochannel open/close valve exploiting thermoresponsive polymer modified on the channel wall was developed, but the response time with temperature change is several minutes, which is slower than the response time of ~1 s required to analytical devices such as immunoassay and chromatography, and the use of valve is limited to reagents without any damage to the polymer.[23]

On the other hand, the use of conventional PDMS valves in nanofluidic devices is also difficult because PDMS nanochannels cannot maintain their shape during pressure-driven fluid control due to the malleability of the material and the high driving pressures utilized. For example, considering Hooke's law, given by $\sigma = E\varepsilon$, where σ is the stress, E is the Young's modulus, and ε is the strain rate, a stress of $\sigma = 10^6$ Pa deforms a 10^2 nm nanochannel made of PDMS ($E = 10^6$ Pa) in 10^2 nm. This means that the amount of deformation of the PDMS nanochannel is comparable to its size when 10^5–10^6 Pa pressure is applied to the nanochannel to drive the liquid at 10^{-1}–10^0 mm/s velocity (10^1–10^2 fL/s flow rate), which is a typical value used in nanofluidic chemical applications.

Therefore, development of 10^1–10^3 nm nanochannel open/close valves fabricated from rigid materials such as glass or plastic is a matter of intense interest in the field of nanofluidics. Herein, we propose an open/close valve for nanochannels that exploits the deformation characteristics of glass, which is the most commonly used material in chemical systems because of its mechanical and chemical stability. Because of their 10^1–10^3 nm smallness, deformations can be used to open/close glass nanochannels in the same way they operate conventional PDMS valves in microfluidics. With that point in mind, this paper

reports on the concept, design, and fabrication of a 308 fL, glass-made valve, the construction of a related valve control system, verification of its related working principle, and demonstration of stopping liquid flow in a nanochannel.

2. Concept and Design

Figure 1 shows the conceptual design of 10^1–10^3 nm nanochannel open/close valve, which operates by exploiting tiny glass deformations. The valve is composed of a shallow circular valve chamber of fL volume, which is wider than a nanochannel, located in the nanochannel and an actuator that, when under certain force, can produce the glass deformation required to open/close the valve. In the closed state, the fluid flow in the nanochannel is stopped. Noted that the circular chamber can minimize the local maximum stress when the glass is deformed: the local maximum stress of the circular chamber is 6.7 times smaller than that of a square chamber, which is approximately estimated from the classical material mechanics.[24] Since the valve chamber is closed by an arc-shaped deflection of the glass substrate, we proposed addition of a multi-stepped nanostructure to the bottom of valve chamber which fits the shape of deflected glass to suppress liquid leakage from remained gap at the closed state.

In order to realize the proposed concept, the following requirements are fulfilled: (i) fL-volume in the valve chamber that is in similar order to the nanochannel volume and (ii) sufficient deformation of the glass by the actuator without breaking it.

Based on the concept above, we designed the proposed valve in order to verify the working principle.

Both the width and depth of nanochannel were designed to be 900 nm. Then we set the valve chamber diameter and depth to $2a$ = 100 μm and z = 70 nm, respectively, and the diameter of the actuator to $2r$ = 25 μm. In order to suppress the liquid leakage in the closed state, we designed the valve chamber with a four-stepped nanostructure (17.5 nm × 4) to create a total chamber volume of ~300 fL. Thus, requirement (i) was satisfied.

To satisfy requirement (ii), we used an analytical theoretical approach to estimate the relationship between stress and deformation for different glass substrate thicknesses in order to determine an appropriate glass thickness for the valve realization purpose. The relationship between stress on the glass σ_m and deformation of the glass y_m can be approximately given by[24]

$$\sigma_m = \frac{3F}{4\pi t_g^2}(1+\nu)\left(\frac{r^2}{a^2} + 2\ln\frac{a}{r} - 1\right) \quad (1)$$

$$y_m = \frac{12(1-\nu^2)F}{8\pi E t_g^3}\left[r^2 \ln\frac{r}{a} + \frac{a^2(a^2-r^2)}{2a^2}\right] \quad (2)$$

where F is the force by the actuator, t_g is the glass thickness and ν is the Poisson ratio. For the deformation part, we used a glass substrate of the Young's modulus of $E = 7.3 \times 10^{10}$ Pa, the Poisson ratio of ν = 0.2 and the breaking strength of 400 MPa as described later. The results of the estimation at various glass thicknesses ranging from 1 to 100 μm are presented in Fig. 2. The proposed valve concept is based on glass deflection into the chamber at a depth of ~70 nm, and the most appropriate thickness for such purpose was determined to be t_g < 100 μm, as is evident from Fig. 2. Taking into account that a sufficient glass deformation value is more than 70 nm at a smaller stress value, as well as considering the ease of handling of glass material, we determined to use a glass substrate of a 45 μm thickness for the valve

realization purposes. The force required to close the valve is calculated from Eq. 2 to be F = 1.1 N. Since the stress on the glass with 70 nm deflection is calculated to be 276 MPa, which is 1.5 times lower than the breaking stress, stable and repeatable use of the valve can be expected.

Accordingly, in case of devices made of glass, the proposed circular, round-bottom valve that is wider than the channel is necessary, while just rounded channels are sufficient to realize fully-closed valves in case of devices made of soft materials like PDMS.[8] In this study, as shown in Fig. 1, the valve chamber has a high aspect ratio of 1423 (width: 100 μm, depth: 70 nm) much wider than the 900 nm square nanochannel, and the round-bottom of the valve chamber was approximately designed by adding the four-stepped nanostructure to the bottom of valve chamber.

Using other rigid materials is considered to achieve more thinner substrate for larger deformation, which is required to realize more deeper valve. However, as described above, availability of other materials is dependent not only on the thickness but also the material properties. For example, silicon nitride can realize a thin substrate more easily than glass, but is more rigid than glass of approximately 4 times higher Young's modulus (E = ~3.0×10^{11} Pa). From Eq. (2), in order to achieve similar deformation to the glass, 1/4 thickness is required. Hence the advantage of using silicon nitride for achieving thinner substrate is cancelled.

In addition, for applying the device to chemical reactions at high temperatures, thermal stability of the valve is required. In case of glasses, since the coefficient of thermal expansion is on the order of 1×10^{6} K^{-1}, the deformation of a 10^{1} μm thickness glass by 100°C temperature difference is calculated to be

1 nm. Considering the depth of valve chamber, influences on the valve performance is negligibly small in the current design. On the other hand, if plastics such as polymethyl methacrylate are used, the deformation by 100°C temperature difference becomes 10 nm because of larger thermal expansion by 1 x 10^6 K^{-1} compared with the glasses, and will affect the valve performances.

2. Experimental

2.1. Fabrication of nanofluidic device with nanochannel open/close valve

Based on the design described above, we developed a fabrication process of the fL-nanofluidic valve on a microchip using the top-down fabrication methods established by our group.[10, 25] Figure 3 shows a fabrication process of the nanochannel open/close valve. The nanochannel and the valve chamber were fabricated on a 0.7-mm-thick fused-silica substrate (70 mm × 30 mm, VIO-SILSX, Shin-Etsu Quartz Co., Ltd., Tokyo, Japan) via a combination of electron beam lithography and dry etching. In the electron beam lithography by ELS-7500 (Elionix, Tokyo, Japan), ZEP-520A (Zeon Corp., Tokyo, Japan) was used as an electron beam resist. The dry etching by NLD-570 (ULVAC Co., Ltd., Kanagawa, Japan) was performed using mixture of CHF_3 and SF_6 gases.

To realize the valve chamber with the four-stepped nanostructure, we repeated a nanofabrication of a circular chamber 4 times with alignment by makers (diameter × depth: 50 μm × 17.5 nm, 72 μm × 17.5 nm, 88 μm × 17.5 nm and 100 μm × 17.5 nm, as shown in Fig. 1).

In the next step, two U-shaped sample injection microchannels (500 μm wide and 7 μm deep) were

fabricated on the same substrate using photolithography and dry etching processes. KMPR® 1035 (Microchem Corporation, MA, USA) was used as a photo resist in the photolithography and the dry etching was performed using mixture of C_3F_8, CHF_3 and Ar gases.[26] The U-shaped microchannels were located on the both sides of the nanochannel containing the valve chamber. Inlet holes were bored through the patterned substrates using a diamond-coated drill.

The micro/nano-fabricated substrate was bonded to a 45 μm borosilicate glass substrate (Nippon Electric Glass Co., Ltd., Tokyo, Japan). Before the bonding, the both substrates were washed in a mixed three-to-one solution of sulfuric acid and hydrogen peroxide. Then the micro/nano-fabricated substrate was ultra-sonicated for 10 min. A low temperature bonding method developed by our group was used for the bonding process.[27] After activating the surface of glass substrates via oxygen and fluorine plasma, the substrates were bonded at the temperature of 65°C and under 5000N pressure for five hours. All operations were carried out in clean rooms (classes 100 and 1000) in order to exclude any impurities during the chip fabrication.

2.2. Valve verification experiments

Figure 4 shows an experimental setup used for principle verification experiments. A valve control system consists of a stainless-steel pin, a piezoelectric (PZT) driven actuator of a 2.3 ms response time and a force sensor (Nano-control Co., Ltd., Tokyo, Japan). All set-ups were constructed as a single body together with the microchip jig in order to prevent any additional vibration. The valve control system was combined with a fluorescence-microscope that was placed on an optical table with an anti-vibration

system. The fabricated microchip was placed on the stainless-steel plate with its thin glass side facing up and secured in place with a jig. Before aligning the actuator to the valve portion, capillaries were connected to the chip. After that, the pin was aligned with the microchip by monitoring through the microscope. A sample solution containing 100 μM fluorescein dissolved into phosphate buffered saline (PBS) was introduced into the inlet microchannel using a pressure controller, and a PBS solution was introduced into the outlet microchannel using another pressure controller. After ensuring that no leakage occurred, we started valve operaton experiments by controlling the actuator and pressure controller as described later. The entire process was monitored through the fluorescence microscope.

3. Results and Discussion

3.1. Fabricated nanofluidic device

Figure 5 shows the fabricated nanofluidic device and valve chamber. The two sets of U-shape microchannels with inlet holes for sample introduction were located on the fused silica substrate and connected separately to the nanochannels that formed two independent devices next to each other on one microchip. The sizes of nanofabricated parts mentioned above were verified by SEM and AFM measurements, respectively, before the chip bonding process, and their sizes were found to be in a good agreement with our valve design. The observation by a nanoscale optical profiler (WYKO NT9100A, Bruker Corp., MA, USA) indicated that the four-stepped nanostructure in the bottom of valve chamber was successfully fabricated with a roughness less than 2 nm. Noted that the low temperature bonding

method of glass substrates could be applied to the bonding of different glass materials, fused-silica and borosilicate.

3.2. Verification of valve open/close by glass deformation

First, we verified the valve open/close operations by the glass deformation and investigated effects of the shape of fL valve chamber. In the experiments, we began valve operation in the open state after filling the nanochannels with the fluorescein solution. The fluorescein solution was injected into the nanochannels and the valve chamber by a pressure of 100 kPa. Then the force by the actuator was added to the glass deformation part and was gradually increased. The average fluorescent intensity at the valve chamber, which is proportional to the volume of gap space, was measured. Noted that the background intensity just near the region of interest was subtracted from the detected image intensity. Since the depth of valve chamber was only 70 nm and the excitation intensity was decreased to reduce fluorescence bleaching, the fluorescent intensity in the valve was low and signal-to-background ratios were 0.7~2. We confirmed that the background intensity was almost uniform. In order to investigate the effect of the chamber shape, the experiments were also conducted for a flat valve chamber without the four-stepped nanostructure.

Figures 6(a) and (b) show captured fluorescent images, and the average fluorescent intensity at the valve chamber as function of the applied force, respectively. As shown in Fig. 6(b), with increasing the applied force, the fluorescent intensity decreases, and reaches to a constant value indicating that the valve was closed by the glass deflection, around the applied force of F = 1.0 N, which approximately

corresponds to the designed force value. Therefore, the concept of nanochannel open/close valve utilizing glass deformation and the design based on the classical material mechanics were validated.

In case of the flat valve chamber without the four-stepped nanostructure, 50% of the fluorescent intensity remains at the closed state (Fig. 6(b)). This indicates that 50% of the chamber space was still open because the corner region couldn't be closed as obviously shown in Fig. 6(a). Even at this condition, the fluid flow is considered to be decreased due to 10^1 times increased fluidic resistance by the narrowed valve chamber, which is roughly estimated from the cross-sectional area, but the leakage by the molecular diffusion cannot be avoided. On the other hand, in case of the valve chamber with the four-stepped nanostructure, the fluorescent intensity drastically decreases to 4% at the closed state (Fig. 6(b)) because the corner region was also closed (Fig. 6(a)). Figure S1 (Supplementary Information) shows profiles of image intensity along the 4-stepped valve chamber at the open and closed states. Although the signal-to-noise ratio is low because the valve depth was only 70 nm even at the deepest part and the fluorescein concentration was 100 μM to avoid the quenching, the result obviously indicates decrease of the volume of fluorescein solution included in the valve chamber with the closing. At this condition, it is expected that the fluid flow is stopped due to 10^4 times increased fluidic resistance, and the leakage by the diffusion is also suppressed. Accordingly, effectiveness of the four-stepped nanostructure on closing the fL valve was successfully verified.

To confirm the stability and durability of the nanochannel open/close valve, we performed repeated auto-controlled valve actuating (open/close) test operation. Because of the long-time monitoring, the

frame interval was set to be 0.66 s. The result of repeated open/close operations at a 180 s period (open duration: 90 s, closed duration: 90 s) is presented as shown in Video S1, and the average fluorescent intensity in the valve chamber is plotted as function of the time that is partially shown in Fig. 7. The measured durations for both open and closed states were 90-91 s which correspond to the experimental conditions. Thereby we succeeded in the valve operation over 50 time without the glass breaking as designed.

3.3. Stop-flow in nanochannel by open/close valve

Next, we applied the valve to stopping/flowing the liquid in the nanochannel. We began valve operation in the closed state by the applied force of $F = 1.05$ N after filling the nanochannels with the PBS solution as an initial state. A 100 kPa pressure was applied to the inlet microchannel in order to inject the fluorescein solution from the inlet microchannel, and then the valve was opened at $t = 179.8$ s.

Figure 8 shows captured fluorescent images and Figure 9 shows the fluorescent intensity of the downstream nanochannel as function of time. In the closed state from $t = 0$ s to $t = 179.8$ s, as shown in Fig. 8, the fluorescein molecules reached to the upstream nanochannel at $t = 60$ s by a small leak flow through the closed valve or diffusion of fluorescein molecules from the inlet microchannel, and the fluorescent intensity in the upstream nanochannel gradually increased. As shown in Fig. S2 (Supplementary Information), the fluorescent intensity at the downstream nanochannel ($x = 0$ μm) is nearly zero at $t = 0$ s and slightly increases at $t = 60$ s. This result suggests that a small amount of fluorescein molecules passed through the closed valve by the small leak flow or the molecular diffusion,

and caused the slightly increased fluorescent intensity. We repeated the experiments and the result shown here is one of the experiments. Hence the fluorescent intensity of nearly zero at t = 0 s suggests that adsorption of fluorescein molecules to the channel wall was negligible.

After the valve open at t =179.8 s, the fluorescein solution was rapidly injected into the downstream nanochannel by the fluid flow and ejected to the outlet microchannel, as shown in Fig. 8 and Video S2. From the fluorescent intensity of the nanochannel at two different points (x = 0 μm and x = 160 μm) as shown in Fig. 9, the flow velocity and the flow rate were calculated to be 0.26 mm/s and 209 fL/s, respectively. The rapid change in fluorescent intensity of the nanochannel suggests a response time of ~0.65 s, which is sufficiently fast for the nanofluidic analytical devices such as immunoassay and chromatography. This response time is considered to be because of a hydraulic resistance with the liquid flow through the opened valve chamber. In this state, there are two pressures to drive the liquid. One is the applied pressure to the nanochannel of 100 kPa. Another is a negative pressure generated by sudden opening of the valve chamber by the actuator. On the other hand, as shown in Fig. 9, the fluorescent intensity at x = 160 μm, which is near the outlet microchannel, is 70% lower than that at x = 0 μm. Since the variation of nanochannel depth is less than 1% as previously reported by our group,[28] main reasons of the 70% difference in the fluorescent intensity are distribution of excitation intensity of fluorescence and diffusion of fluorescein molecules to the outlet microchannel filled with the PBS solution. From rough estimation using the fluorescent intensities at the upstream nanochannel where the fluorescein concentration is constant, heterogeneity of excitation intensity was approximately 20%. Hence the

remaining 50% difference is because of decrease of the fluorescent intensity by the diffusion of fluorescein molecules to the outlet microchannel.

In the closed state just before the valve open (t = 177 s), as shown in Fig. 9, the fluorescent intensity of the downstream nanochannel (x = 0 μm) is only 0.6% of that at the open state (t = 182 s), which indicates the liquid flow in the nanochannel was stopped because the valve chamber with the four-stepped nanostructure was closed by the glass deflection.

We further evaluated sealing properties of the valve at the closed state as function of the applied pressure. The experiments were conducted at applied pressures ranging from 100 kPa to 490 kPa. We began valve operation in the closed state after filling the nanochannels with the PBS solution as an initial state, and the pressure was applied to inject the fluorescein solution. The valve worked without breaking even at the pressure of 490 kPa. In order to evaluate the sealing at the closed state, as well as above discussion, the ratio of the fluorescent intensity in the downstream nanochannel (x = 0 μm) at the closed state to that at the open state was evaluated. Figure 10 shows the ratio of fluorescent intensity as function of the applied pressure. As the pressure increases to 490 kPa, the fluorescent intensity in the downstream nanochannel increases and reaches to ~2.4% of that at the open state. This result suggests that a small leak flow through the closed valve occurred but was still sufficiently small at 490 kPa compared to the flow at the open state. The leak flow can be further suppressed by increasing the number of steps at bottom of the valve chamber to decrease remained space at the closed state. Therefore, we verified the stop-flow in the nanochannel by the fL-valve.

Accordingly, we succeeded in stopping/flowing the liquid in the nanochannel by the open/close valve exploiting nanoscale glass deformation with performances required to the nanofluidic analytical devices for the first time. Although suppressing the molecular-scale leakage on the hydrophilic glass surface is still difficult, our nanochannel open/close valve is useful in nanofluidics of fL volumes (10^2–10^3 nm space sizes). The developed valve is quite important to achieve sophisticated fluid control in micro/nanofluidic devices made of glass as well as the PDMS valves.

In addition, recent studies including those reported by our group have suggested high performances of nanofluidics. For example, exploiting fL volumes for immunoassay realized analysis of single/countable protein molecules.[15] Utilizing a nanochannel as separation column achieved more than 10^4 plate numbers of chromatographic separation.[16] In addition, a fL-sampling interface from living single cell was realized.[28] The developed valve will greatly contribute to integration of these nanofluidic chemical operations to realize novel applications such as single cell proteomics.

For the integration of the fL-valves on a microchip, using commercial miniaturized piezo electric actuators is possible. If the glass thickness decreases to 10^0 nm or complicated fabrication techniques for three-dimensional nanostructure and functional materials are developed, several miniaturized mechanics for the deflection such as cantilever, thermpneumatic and electromagnetic, which are reported in previous studies,[21, 29] can be applied to realize more dense integration. However, for using the fused silica base where micro- and nanochannels are fabricated, bonding of deformation materials to the fused silica base is required. Since we succeeded in the bonding of fused silica glass and borosilicate glass which has

silanol groups on the surface required for the bonding method,[27] other glasses such as Gorilla glass of higher breaking strength and materials having silanol groups on the surface are considered to be available.

4. Conclusions

In this study, we proposed the concept and design of an open/close valve consisting of 10^1–10^3 nm nanochannels that exploits tiny deformation of glass. The fL-volume valve chamber was designed based on an analytical model of the expected material deformation. In addition, we fabricated the four-stepped nanostructure in the bottom of valve chamber which fits the arc-shape of deflected glass to sufficiently close the valve for preventing the leakage. The working principle behind the valve concept was experimentally confirmed. We presented a principle verification of a 308 fL volume valve on a microchip made of glass, confirmed stability and durability during 50 repeated valve open/close operations, and succeeded in stopping/flowing the liquid at 209 fL/s (0.29 mm/s) under a 100 kPa pressure in a 900 nm nanochannel with a fast response of ~0.65 s. A leak flow from the closed valve was sufficiently small even at a 490 kPa pressure.

This work provides the first verified open/close operations of a fL-volume valve made of glass having performances required to the nanofluidic analytical devices. Since, like a conventional microfluidic PDMS valve, this valve does not require any surface chemical modifications, nor any nanomaterials and thermal/electrical controls, it can be applied to a wide variety of chemical applications, such as biochemical analysis and chemical synthesis. Furthermore, the methodology can be applied to

nanofluidic devices made of other rigid materials such as plastic. The results can be expected to contribute significantly to the fabrication of novel integrated nanofluidic chemical systems for various fields such as single molecule analytical chemistry and single cell proteomics.

Conflicts of Interest

There are no conflicts of interest to declare.

Acknowledgement

The authors gratefully acknowledge the financial support from the Core Research for Evolutional Science and Technology (CREST) of the Japan Science and Technology Agency (JST): JPMJCR14G1.

References

1 K. Mawatari, Y. Kazoe, A. Aota, T. Tsukahara, K. Sato and T. Kitamori, *J. Flow Chem.*, 2011, **1**, 3-12.

2 G. M. Whitesides, *Nature*, 2006, **442**, 368-373.

3 M. Tokeshi, T. Minagawa, K. Uchiyama, A. Hibara, K. Sato, H. Hisamoto and T. Kitamori, *Anal. Chem.*, 2002, **74**, 1565-1571.

4 M. A. Unger, H.-P. Chou, T. Thorsen, A. Scherer and S. R. Quake, *Science*, 2000, **288**, 113-116.

5 D. J. Beebe, J. S. Moore, J. M. Bauer, Q. Yu, R. H. Liu, C. Devadoss and E.-H. Jo, *Nature*, 2000,

404, 588-590.

6 G. Takei, M. Nonogi, A. Hibara, T. Kitamori, H.-B. Kim, *Lab Chip*, 2007, **7**, 596-602.

7 T. Thorsen, S. J. Maerkl, S. R. Quake, *Science*, 2002, **298**, 580-584.

8 J. Melin, S. R. Quake, *Annu. Rev. Biophys. Biomol. Struct.*, 2007, **36**, 213-231.

9 K. A. Shalkh, K. S. Ryu, E. D. Goluch, J.-M. Nam, J. Liu, C. S. Thaxton, T. N. Chiesl, A. B. Barron, Y. Lu, C. A. Mirkin, C. Liu, *PNAS*, 2005, **102**, 9745-9750.

10 K. Mawatari, Y. Kazoe, H. Shimizu, Y. Pihosh and T. Kitamori, *Anal. Chem.*, 2014, **86**, 4068-4077.

11 A. Hibara, T. Saito, H.-B. Kim, M. Tokeshi, T. Ooi, M. Nakao and T. Kitamori, *Anal. Chem.*, 2002, **74**, 6170-6176.

12 K. Shirai, K. Mawatari and T. Kitamori, *Small*, 2014, **10**, 1514-1522.

13 H. Chinen, K. Mawatari, Y. Pihosh, K. Morikawa, Y. Kazoe, T. Tsukahara and T. Kitamori, *Angew. Chem. Int. Ed.*, 2012, **51**, 3573-3577.

14 H. Shimizu, K. Mawatari and T. Kitamori, *Anal. Chem.*, 2010, **82**, 7479-7484.

15 K. Shirai, K. Mawatari, R. Ohta, H. Shimizu and T. Kitamori, *Analyst*, 2018, **143**, 943-948.

16 R. Ishibashi, K. Mawatari and T. Kitamori, *Small*, 2012, **8**, 1237-1242.

17 C. Wang, Y. Kazoe, K. Morikawa, H. Shimizu, Y. Pihosh, K. Mawatari and T. Kitamori, *RSC. Adv.*, 2017, **7**, 50591-50597.

18 Y. Pihosh, J. Uemura, I. Turkevych, K. Mawatari, Y. Kazoe, A. Smirnova, T. Kitamori, *Angew. Chem. Int. Ed.*, 2017, **56**, 8130-8133.

19 R. Arayanarakool, L. Shui, S. W. M. Kengen, A. van den Berg and J. C. T. Eijkel, *Lab Chip*, 2013, **13**, 1955-1962.

20 B. R. Cipriany, P. J. Murphy, J. A. Hagarman, A. Cerf, D. Latulippe, S. L. Levy, J. J. Benítez, C. P. Tan, J. Topolancik, P. D. Soloway and H. G. Craighead, *PNAS*, 2012, **109**, 8477-8482.

21 S. D. Solares, M. Blanco, W. A. Goddard III, *Nanotechnology*, 2004, **15**, 1405-1415.

22 K. Mawatari, S. Kubota, Y. Xu, C. Priest, R. Sedev, J. Ralston and T. Kitamori, *Anal. Chem.*, 2012, **84**, 10812-10816.

23 Y. Xu, M. Shinomiya, A. Harada, *Adv. Mater.*, 2016, **28**, 2209-2216.

24 S. Timoshenko and S. Woinowsky-Krieger, *Theory of Plates and Shells*, McGraw-Hill, 1964.

25 T. Tsukahara, K. Mawatari, A. Hibara and T. Kitamori, *Anal. Bioanal. Chem.*, 2008, **391**, 2745-2752.

26 K. Morikawa, K. Matsushita, T. Tsukahara, *Anal. Sci.*, 2017, **33**, 1453-1456.

27 Y. Xu, C. Wang, L. Li, N. Matsumoto, K. Jang, Y. Dong, K. Mawatari, T. Suga and T. Kitamori, *Lab Chip*, 2013, **13**, 1048-1052.

28 L. Lin, K. Mawatari, K. Morikawa, Y. Pihosh, A. Yoshizaki, T. Kitamori, *Analyst*, 2017, **142**, 1689-1696.

29 P. Gravesen, J. Branebjerg and O. S. Jensen, *J. Micromech. Microeng.*, 1993, **3**, 168-182.

Figure Captions

Figure 1. Conceptual design of the proposed nanochannel open/close valve made of glass consisting of nanochannel, fL shallow valve chamber and actuator. Cross sectional views show the valve functionality: open and closed under applied force by the actuator. Noted that the vertical and horizontal scales are different.

Figure 2. Relationship between stress and deflection for various glass thicknesses, which is calculated from the analytical material deformation model.

Figure 3. Fabrication process of a microchip containing microchannels, nanochannels and a shallow valve chamber with four-stepped nanostructure.

Figure 4. Schematic illustration of an experimental setup consisting of a piezoelectric driven actuator, the fabricated microchip, pressure controllers and a fluorescent microscope.

Figure 5. Photo of the fabricated microchip with two integrated 308 fL-valves. Image below shows the valve chamber with the four-stepped nanostructure, which is connected to the nanochannels, observed by an optical profiler).

Figure 6. Demonstration of the valve principle verification. (a) Fluorescence pictures of the valve area at the open/closed states for the flat valve chamber and the valve chamber with the four-stepped bottom. (b) The average fluorescent intensity at the valve chamber area as function of the applied force by the actuator. Noted that the fluorescent intensity was obtained by subtracting a background intensity from the image intensity, and the fluorescent intensities at the nanochannel overlapped with the valve chamber region were not included.

Figure 7. The fluorescent intensity-time profile at the valve chamber area in the repeated operations of the fL-valve at a 180 s period (open duration: 90 s, closed duration: 90 s). Noted that the fluorescent intensity was obtained by subtracting a background intensity from the image intensity.

Figure 8. Results of stop-flow experiments for the nanochannel utilizing the fL-valve. Fluorescence pictures of the valve operation changing from the closed state to the open state.

Figure 9. The fluorescent intensity-time profile of the valve operation changing from the closed state to the opens state at two detection points at downstream nanochannel (x = 0 μm and x = 160 μm, as shown in an illustration in Fig. 8). Noted that the fluorescent intensity was obtained by subtracting a background intensity from the image intensity.

Figure 10. Ratio of fluorescent intensity of the downstream nanochannel (x = 0 μm) at the closed state to that at the open state as function of the applied pressure. Noted that the fluorescent intensity was obtained by subtracting a background intensity from the image intensity. The fluorescent intensity ratio reaches to 100% at the open state. The error of ±1.4% was calculated from the image noise.

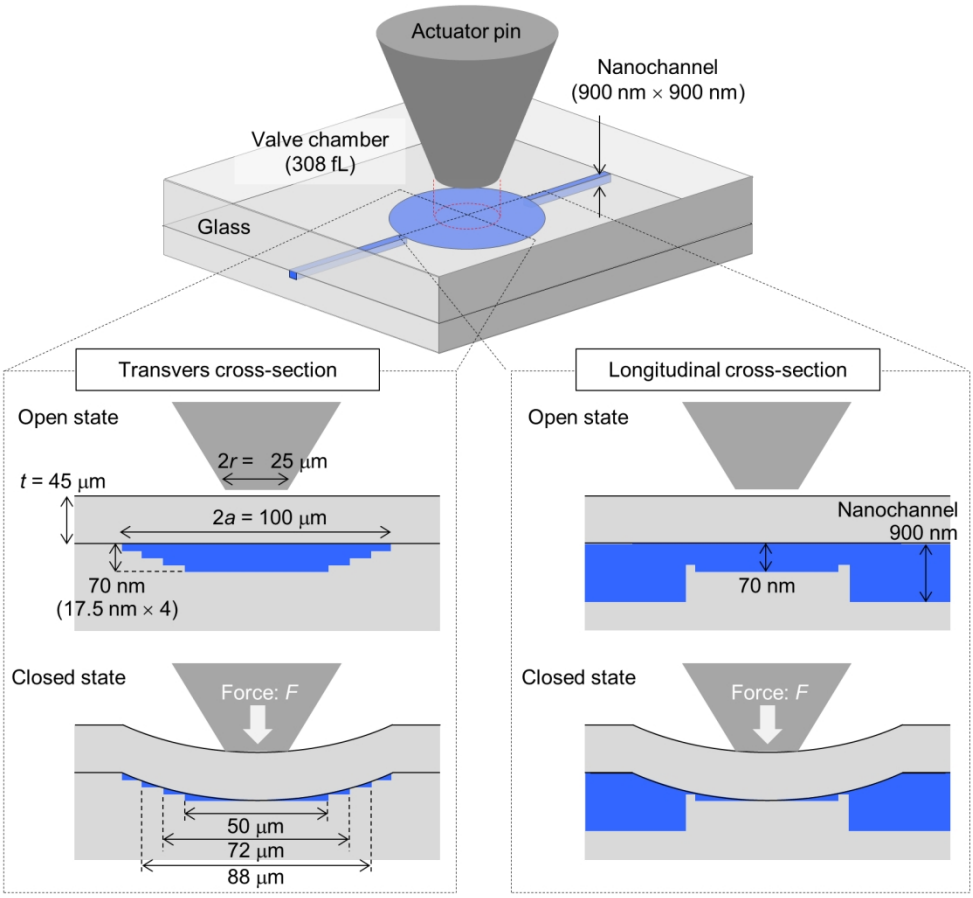

Figure 1

154x138mm (300 x 300 DPI)

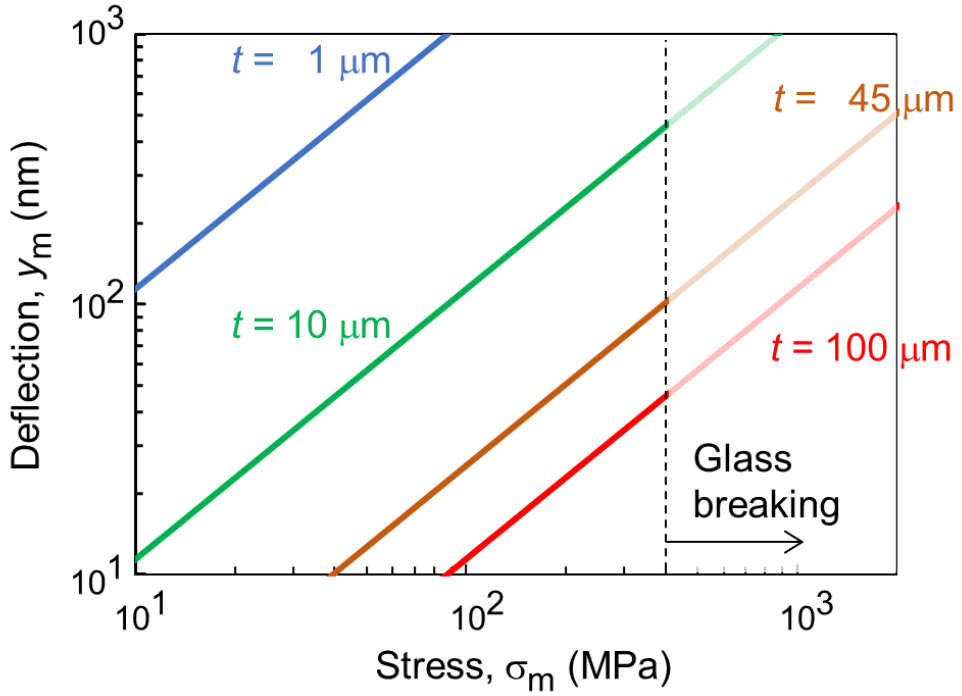

Figure 2

82x59mm (300 x 300 DPI)

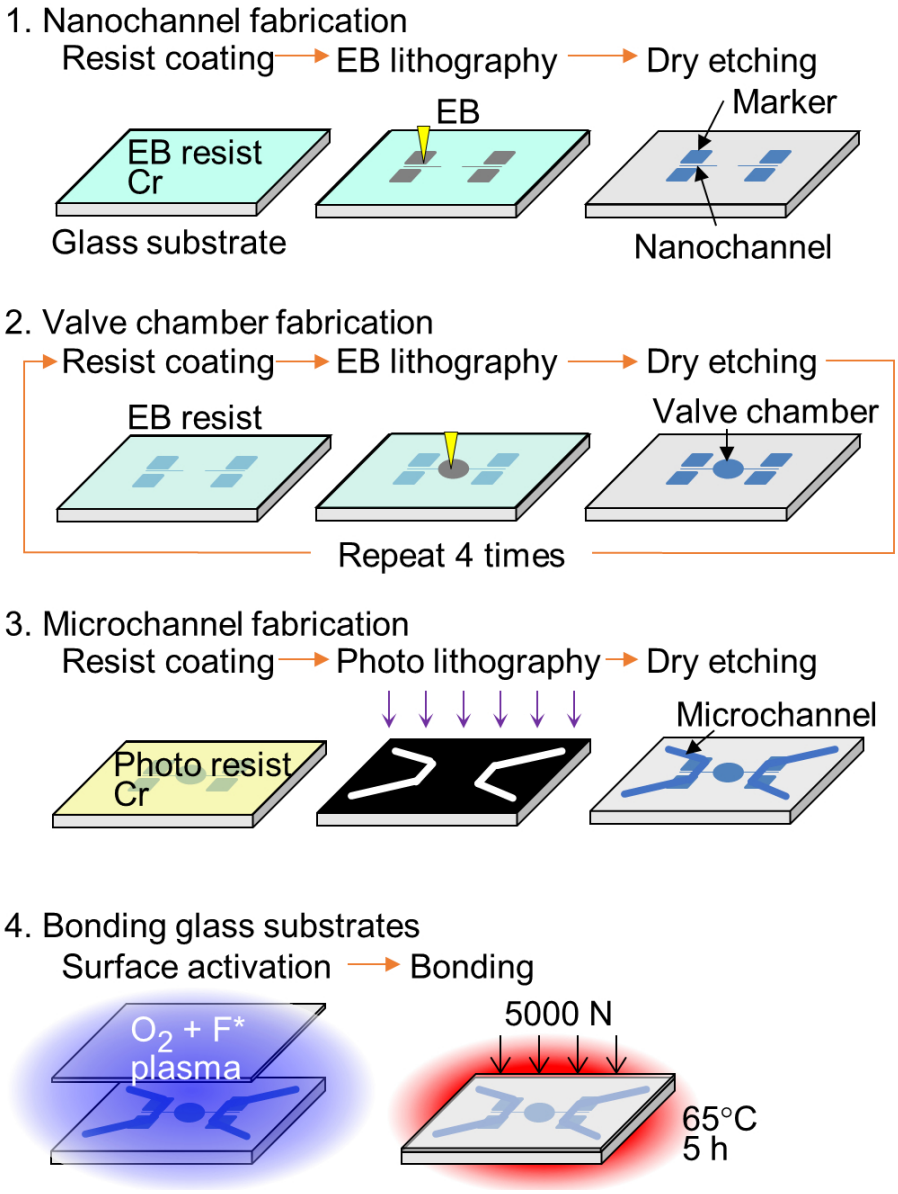

Figure 3

85x113mm (300 x 300 DPI)

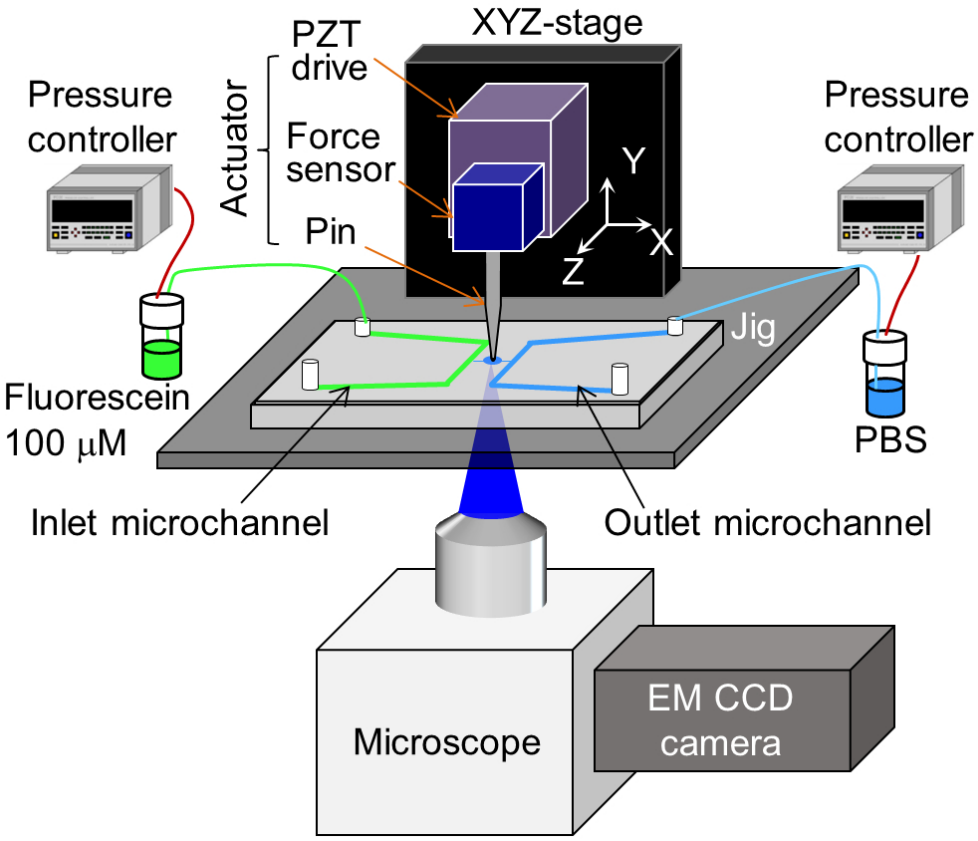

Figure 4

85x72mm (300 x 300 DPI)

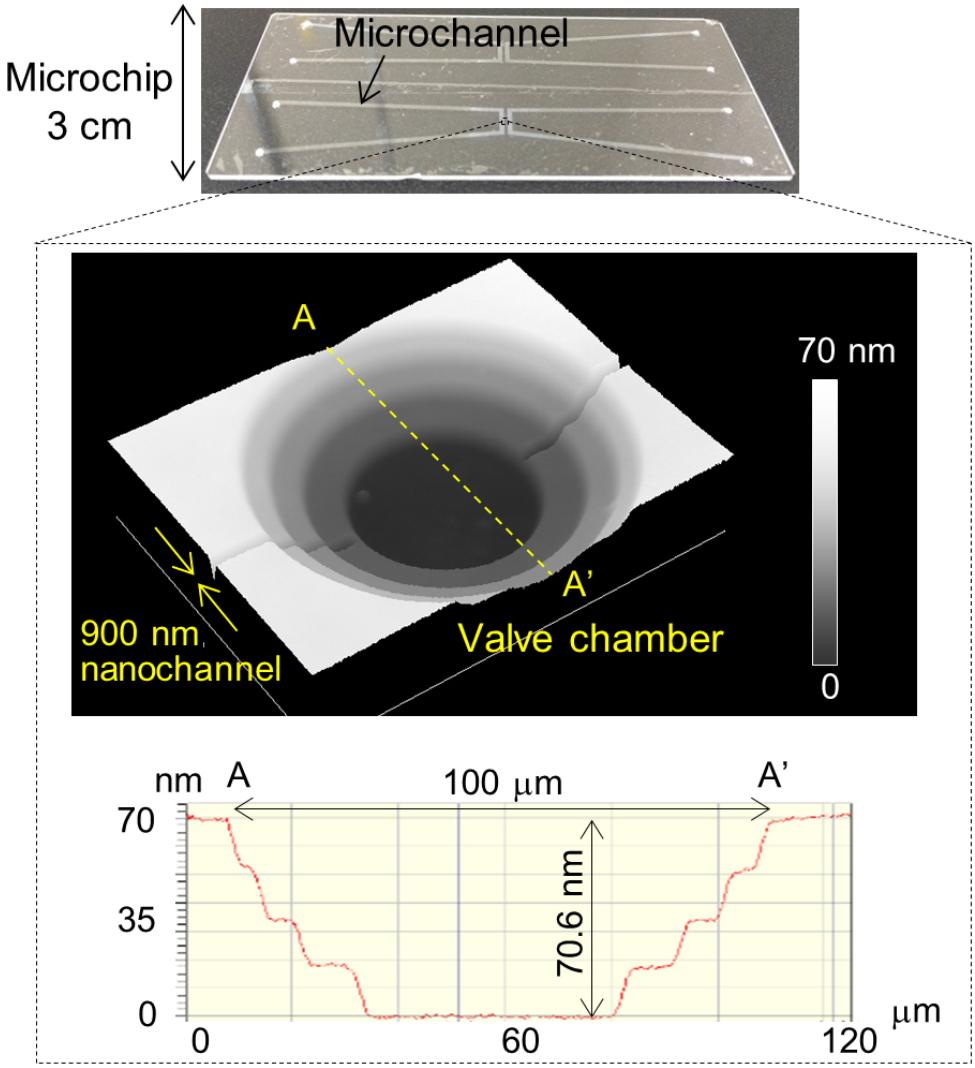

Figure 5

78x85mm (300 x 300 DPI)

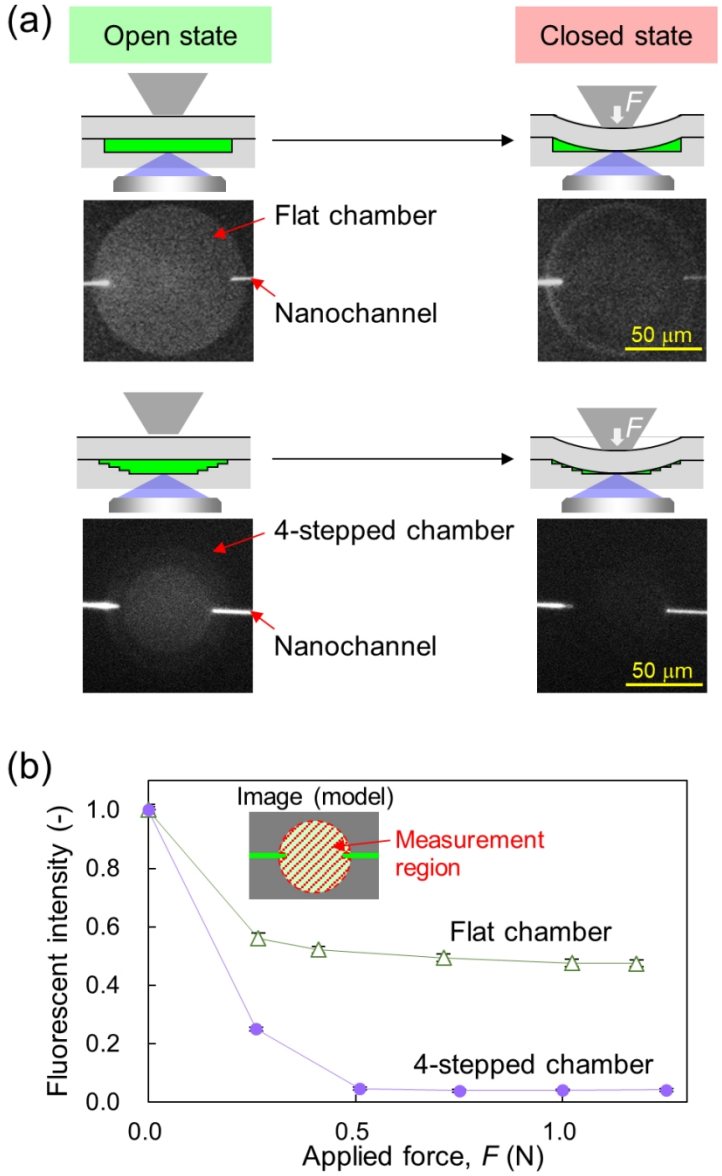

Figure 6

83x135mm (300 x 300 DPI)

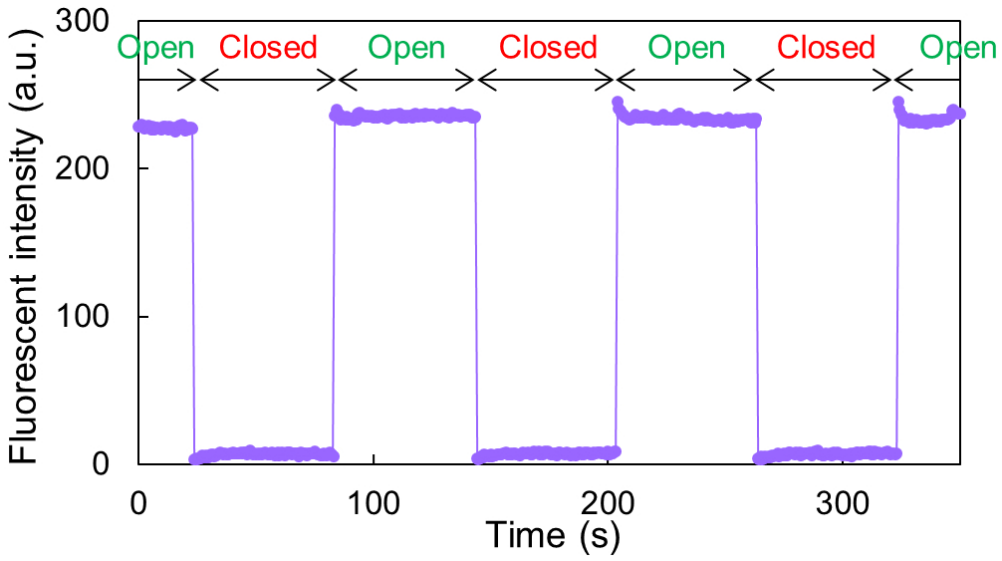

Figure 7

85x48mm (300 x 300 DPI)

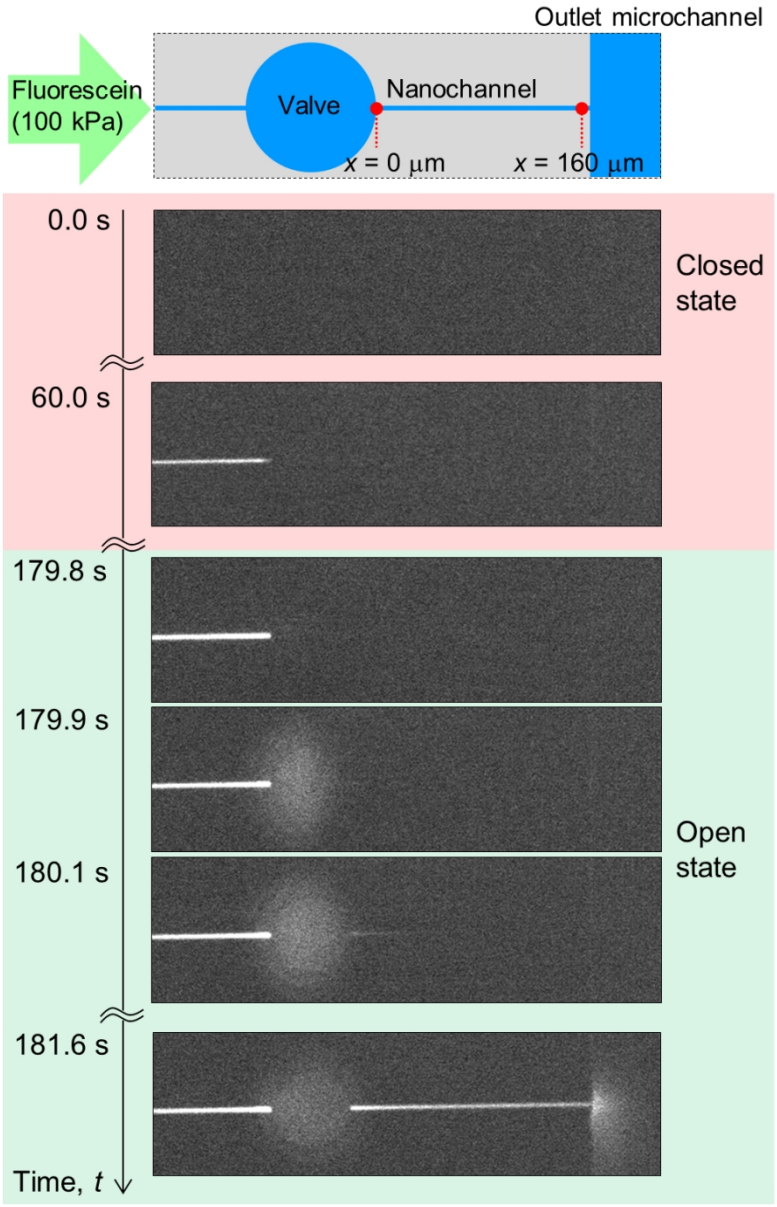

Figure 8

85x129mm (300 x 300 DPI)

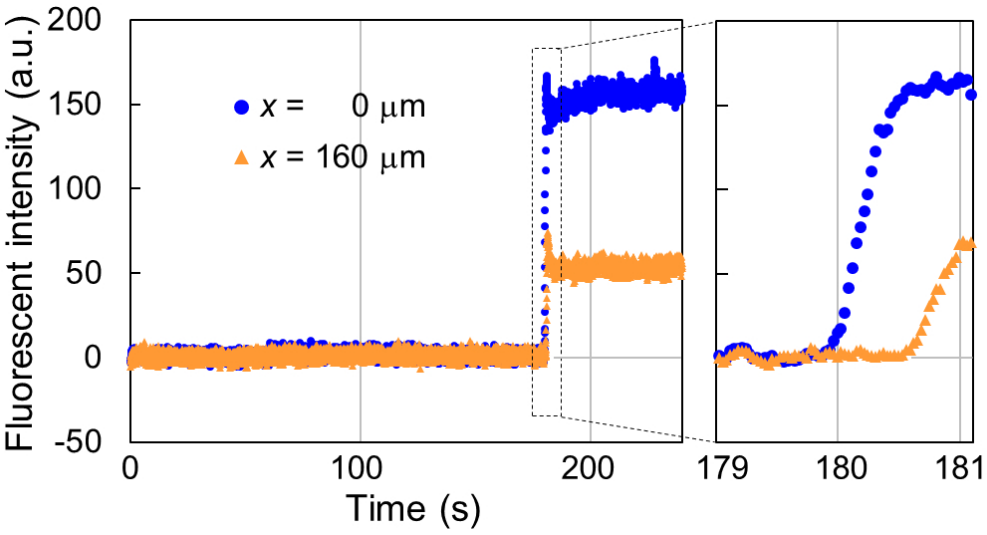

Figure 9

85x44mm (300 x 300 DPI)

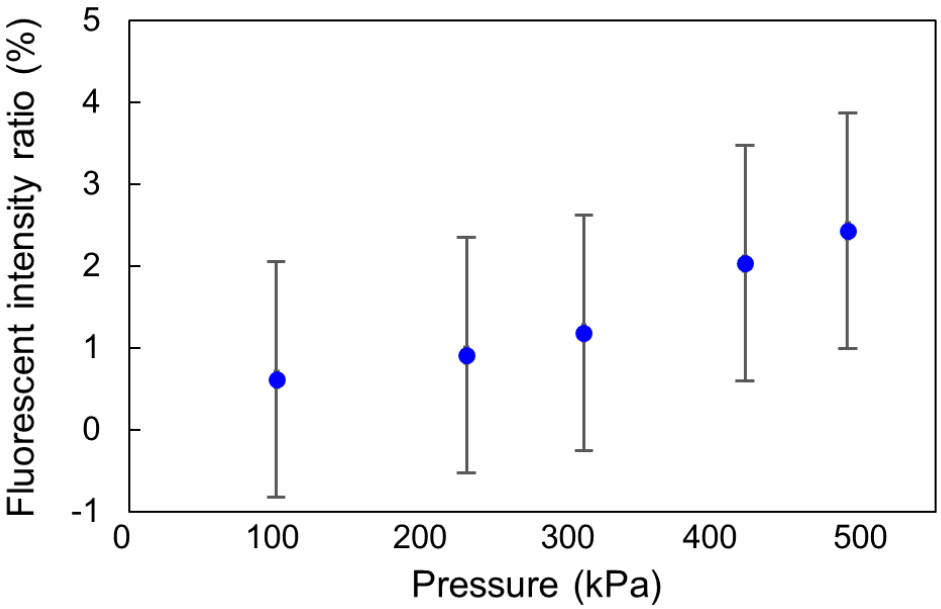

Figure 10

83x53mm (300 x 300 DPI)